JOURNAL OF GEOPHYSICAL RESEARCH, VOL. 100, NO. B4, PAGES 6213–6224, APRIL 10, 1995

Tidal flexure at ice shelf margins

David G. Vaughan

British Antarctic Survey, Natural Environment Research Council, Cambridge, England

Abstract. Hinge zones accommodate the differential tidal movement between floating ice shelves, which move with the sea tide, and grounded ice sheets, which do not. Observations on Rutford Ice Stream and Ronne Ice Shelf, Antarctica, using the kinematic method of Global Positioning System, have yielded the first continuous tidal displacement profiles from an ice sheet hinge zone. The form of these tidal displacement profiles indicates that the flexure can be fit to an elastic beam model using a parameter space optimization technique. The model matches the observed tidal deflection profile to within 5 cm which is similar to the observational uncertainty. The same model and parameter fitting technique is then successfully applied to various other published and unpublished tidal displacement data from Doake Ice Rumples, Bach Ice Shelf, and Ekström Ice Shelf, Antarctica, and Jakobshavns Glacier, Greenland. I conclude that the elastic beam model with a single value of the elastic modulus (0.88 ± 0.35 GPa) adequately describes almost all the data and so can usefully be applied elsewhere. Earlier studies of tidal dissipation in ice shelf hinge zones, based on a viscous or transient creep rheology, showed that perhaps 30% of global tidal energy dissipation could be occurring in ice shelf hinge zones. This study suggests, however, that an elastic rheology may be equally appropriate, in which case this estimation of the tidal energy dissipation is excessively high.

Introduction

Ice Shelf Hinge Zones

Between a grounded ice sheet and a floating ice shelf there is a hinge zone that is neither fully one nor the other. Whereas the grounded ice sheet is supported by its bed and is unaffected by the sea tides, the ice shelf is floating and is in constant motion following the sea tide. The ice within the hinge zone is supported partly by the hydrostatic pressure from the sea beneath and partly by internal stresses. The hinge zone thus accommodates differential movement and suffers cyclic flexure at the tidal frequency. The sea bed topography and the ability of the ice to support stresses over periods of the tidal cycle governs the extent and nature of the hinge zone.

Tidal flexure in ice shelf hinge zones is important to a number of fields of study. It has been suggested that significant power is dissipated from the global tidal system in ice shelf hinge zones [*Doake*, 1978], but to calculate the magnitude of the dissipation we must first determine the rheology governing the flexing.

Glacier fabrics developed by accumulated strain in active zones have been shown to affect the tertiary flow of ice [*Budd and Jacka*, 1989]. Repeated straining in hinge zones could similarly develop ice fabrics which may influence ice shelf flow. The nature of a fabric developed by the ice in the hinge zone would depend on the mechanism and magnitude of the ice shelf flexure.

Synthetic aperture radar interferometry from the ERS 1 satellite can now be used to measure ice sheet velocities from space [*Goldstein et al.*, 1993]. In the hinge zone and over floating ice, however, flow velocities are obscured by tidal displacements, which must be modeled and removed before the flow velocities can be evaluated.

Holdsworth [1977] linked ice shelf evolution directly to sea tides. He suggested that large tidal ranges may inhibit the growth of ice tongues and laterally unbounded ice shelves by generating high stresses at the grounding line. By analyzing the distribution of ice shelves in relation to tidal range, he determined an upper limit for the viability of such ice shelves. This influence should not be overemphasized, however, since the argument is not applicable to the embayed ice shelves which fringe most of the Antarctic continent. Furthermore, he did not account for the climatic limit on ice shelf viability which has recently been shown to have a major influence on ice shelf distribution [*Doake and Vaughan*, 1991].

In this study I present new data gathered on the tidal displacement profile across grounding lines using the kinematic Global Positioning System (GPS) technique. The observations are modeled using elastic beam theory, and the value of the elastic modulus is derived. In the second part of the paper I attempt to harmonize my results with data from other sites using the same modeling technique. I show that elastic flexure adequately explains the observations, given a well-chosen elastic modulus. This simple model of flexure is thus widely applicable, and I discuss the implications for some of the fields of study outlined above.

Previous Field Observations of Hinge Zones

Observations of tidal flexing were originally made on Maudheim Ice Shelf (Figure 1) by *Robin* [1958] using optical leveling. Robin showed that the positions of surface cracks (strand cracks) which were found to open and close

Paper number 94JB02467.
0148-0227/95/94JB-02467$05.00

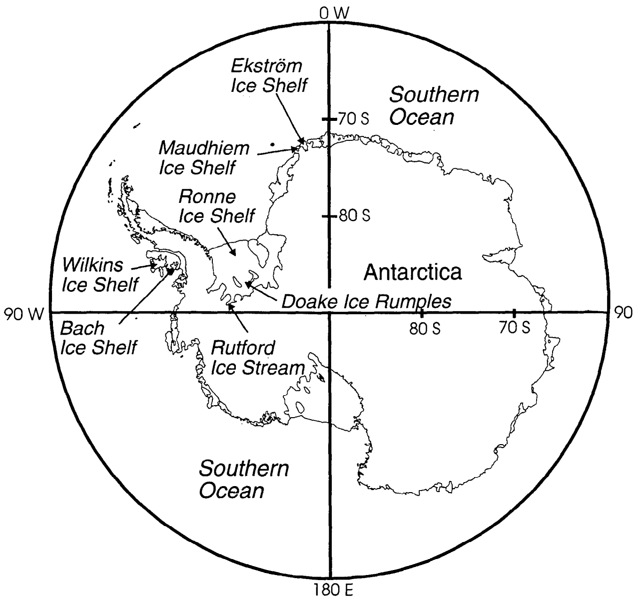

Figure 1. Antarctic location diagram.

with every tide coincided with the position of the maximum stress calculated by considering the ice shelf as a thin elastic beam resting on an inviscid liquid. Since then other authors have used similar equations to match optical measurements of ice shelf deflection [*Lingle et al.*, 1981] and observations of the associated surface tilt [*Stephenson*, 1984; *Smith*, 1991; *Kobarg*, 1988]. Most of these studies have followed Robin and attempted to model the flexure of ice using the simple elastic model. Some elaborations have however, been included to improve the model fit, notably *Holdsworth's* [1977] extension to a viscous and transient creep rheology. The major limitation has always been the poor understanding of the correct constitutive relation for ice at tidal frequencies. Most authors have opted to take elastic moduli from static or instantaneous laboratory tests, and a wide range of values have been used (Table 1). There have thus been a number of studies based on data from single locations, but a comparative study using observations from a variety of locations has not been previously attempted.

Laboratory Studies of Ice Rheology

Natural glacier ice has a complex polycrystalline structure that can deform by many processes that occur either within the crystal (e.g., dislocation glide, elastic deformation) or at crystal boundaries (e.g., grain boundary recrystallization, fracture). All the mechanisms of deformation are present in ice sheets, with some subset being dominant at any one point and on any particular timescale. Since modeling the flow of an ice sheet relies on a good knowledge of ice rheology, much effort has been made to determine the dominant flow mechanism over various timescales in various stress regimes. This has proved to be a difficult task, and our understanding is far from complete; some of the models in current use are incompatible. Useful summaries have been presented by *Hutter* [1983] and by *Budd and Jacka* [1989]. Budd and Jacka, having reviewed data available on ice deformation, arrived at a relatively simple model that could be applied to ice sheet models. The overall deformation was modeled in terms of several component mechanisms acting in series. They stated that on loading the first response of the ice is an instantaneous elastic deformation. This is fully recoverable and increases approximately linearly with stress from 0.024% at 200 kPa to 0.3% at 2.5 MPa, implying an elastic modulus of 0.83 GPa. They found this elastic deformation has little dependence on temperature. After the elastic impulse, primary creep was found to dominate up to 1% strain. This strain was recoverable but delayed and so anelastic. At higher strains nonrecoverable deformation dominates, progressing through primary, secondary, and tertiary creep.

In order to determine the dominant deformation mechanism for tidal flexing according to the Budd and Jacka model, we must determine roughly the strains involved. We need only consider typical values; tidal amplitude (3-5 m) and width of the hinge zone (1-10 km). It will become apparent from the observations discussed later that these are indeed realistic estimates. If the tidal flexure were taken up by a linear displacement, then these figures imply strains of the order of 10^{-6} to 10^{-5}. Over the short time periods of the tidal cycle these strains are very small and likely to be well within the elastic phase reported by *Budd and Jacka* [1989]. It is thus reasonable to attempt to analyze tidal flexure in terms of such an elastic rheology.

Sinha [1978] distinguished between the elastic (Young's) modulus that can only be measured at high frequencies and the effective elastic modulus that is a combination of the truly elastic and viscoelastic response that depends on load time and temperature. He also commented that after loading there is a limited period (of around 1 s) that ice can be considered as a purely elastic material. Although Sinha only presented data for loading frequencies of 10^{-3} to 10^{6} Hertz, extrapolating his data to tidal frequencies (2.5×10^{-5} Hz) suggests an elastic modulus of between 1 and 3 GPa.

Elastic Beam Model

Various solutions of differential equations describing the deformation of an elastic beam have been widely discussed

Table 1. Comparison of the Properties of Ice Used in Various Studies

Source	E, GPa	υ	Reference
	Field Studies		
Rutford Ice Stream, grounding zone	9. 1.8	0.3	*Stephenson* [1984] *Smith* [1991]
Doake Ice Rumples	1.1	0.3	*Smith* [1991]
Ekström Ice Shelf	2.7	0.3	*Kobarg* [1988]
Jakobshavns Isbrae	8.8	0.3	*Lingle et al.* [1981]
Maudheim Ice Shelf	10.	0.3	*Robin* [1958]
	Laboratory Studies		
	1-3		*Sinha* [1978]
	0.83		*Budd and Jacka* [1989]
	9.2-9.4	0.314	*Hutter* [1983] (p. 62)

in relation to a number of geodynamical problems, most notably the flexure of the Earth's lithosphere on geological timescales [e.g., *Turcotte and Schubert* 1982; *McAdoo et al.*, 1978; *Watts et al.*, 1975; *Hetényi*, 1946], as well as for ice flexure [e.g. *Holdsworth*, 1969, 1977]. The dominant forces during small displacements of a thin elastic beam or sheet are the longitudinal extension and compression that occur above and below a notional neutral surface (Figure 2). The problem was analyzed by *Holdsworth* [1969] in the absence of any mean longitudinal stress, and he showed that the problem could be written.

$$D\frac{\partial^4 w}{\partial x^4}=\rho_{sea}\, g[A_0(t)-w(x)] \qquad (1)$$

where the x axis is horizontal and orthogonal to the grounding line, $A_0(t)$ is the level of the ice shelf surface if it were floating in local hydrostatic equilibrium (varying with time due to the tidal oscillation), $w(x)$ is the vertical displacement of the ice sheet surface from the mean position, ρ_{sea} is the sea water density, g is the gravitational acceleration, and D is the flexural rigidity which is given by

$$D=\frac{Eh^3}{12(1-\nu^2)} \qquad (2)$$

where E is the elastic (Young's) modulus, ν is Poisson's Ratio and h the thickness of the ice shelf.

For an ice shelf hinge zone (1) is solved by considering a condition at the grounding line (w=0 and $\partial w/\partial x$=0 at x=0), and a free floating condition beyond the hinge zone ($w=A_0(t)$ at $x=\infty$), where $A_0(t)$ represents the tidal displacement beyond the influence of the hinge zone. The solution for the deflection w is

$$w=A_0(t)[1-e^{-\beta x}(\cos\beta x+\sin\beta x)]. \qquad (3)$$

The parameter β incorporates both the spatial frequency of the flexure and its decay length and is given by

$$\beta^4=3\rho_{sea}\, g\frac{1-\nu^2}{Eh^3}. \qquad (4)$$

The spatial wavenumber, β, will thus be relatively insensitive to changes in E and ν but will have a stronger (although still not linear) dependence on the thickness (h).

Kinematic GPS Measurements From Rutford Ice Stream, Antarctica

Rutford Ice Stream is around 30 km wide, 150 km long, and 2000 m thick. It drains the West Antarctic Ice Sheet into Ronne Ice Shelf through a bedrock trough between the Ellsworth Mountains and Fletcher Promontory. In January

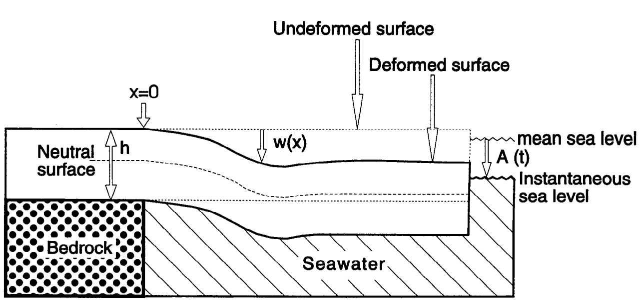

Figure 2. Model of the vertical section through an ice shelf grounding zone. After *Holdsworth* [1969].

1993 I conducted investigations using kinematic GPS on Rutford Ice Stream and nearby on Ronne Ice Shelf. The first site straddled the ice stream grounding line and the second straddled an ice shelf margin. Details of field techniques and overall structural conclusions have already been described [*Vaughan*, 1995] and are only briefly summarized below.

Kinematic GPS for Tidal Flexure

"Kinematic GPS" [*Hofmann-Wellenhof et al.*, 1992] is one of the high-precision "carrier-phase GPS" techniques that are now well established and routinely applied in commercial and research applications [e.g., *Whillans et al.*, 1990; *Minkle*, 1989; *Remondi*, 1985]. Kinematic GPS is used to determine the trajectory of a moving ("rover") GPS receiver with reference to a nominally fixed ("base station") receiver with an achievable precision of a few centimeters.

In this investigation the base station was selected at a location expected to be well above the grounding zone and marked by a tripod that remained fixed throughout the duration of the experiment. From here routes across the grounding zone and out onto the floating ice shelf were established. Several kinematic GPS profiles were collected along exactly the same route from grounded to floating ice at various states of the tide. The differences between the elevation profiles is mostly due to the effect of tidal displacement.

Rutford Ice Stream Grounding Line

Along the centre line of Rutford Ice Stream the grounding zone is pinned at a bedrock step that creates a surface knoll easily visible on some satellite imagery. Conventional studies of the grounding zone of Rutford Ice Stream, using tiltmeters, have already been presented by *Stephenson* [1984] and *Smith* [1991]. These studies have located the position of the flexing limit and have roughly established the extent of the hinge zone.

The model used here was applied by both *Stephenson* [1984] and *Smith* [1991] with varying success. Stephenson used a very high elastic modulus (Table 1) and so had to resort to a "reduced" ice thickness (around 58% of the true value). Smith, however, used a more realistic value of the elastic modulus and found that he did not need a reduced ice thickness to adequately match the observed data.

Three sets of "kinematic" GPS profiles were collected across the grounding zone of Rutford Ice Stream along tracks marked A-A', A-A'', and A-A''' in Figure 3. The roving antenna was mounted on a frame rigidly fixed to the chassis of a snowmobile. Unfortunately, access to the summit of the knoll area is limited by crevassing, and the first 1300 m of track from site A was the same for all three profiles. Good coincidence of the profiles was achieved by driving the snowmobile in the track left from the previous session. The elevations and times along the profiles were then linearly interpolated. The difference between the elevations shows the vertical tidal displacement of the ice shelf (Figure 4).

Inspection of the calculated trajectory from periods when the snowmobile was stationary shows the uncertainty in elevation due to the kinematic GPS method alone to be around ±3 cm. This figure includes both the observation error and the uncertainty introduced by the postprocessing. From repeated profiles on grounded ice I estimate that the method of mounting and driving introduces a further uncer-

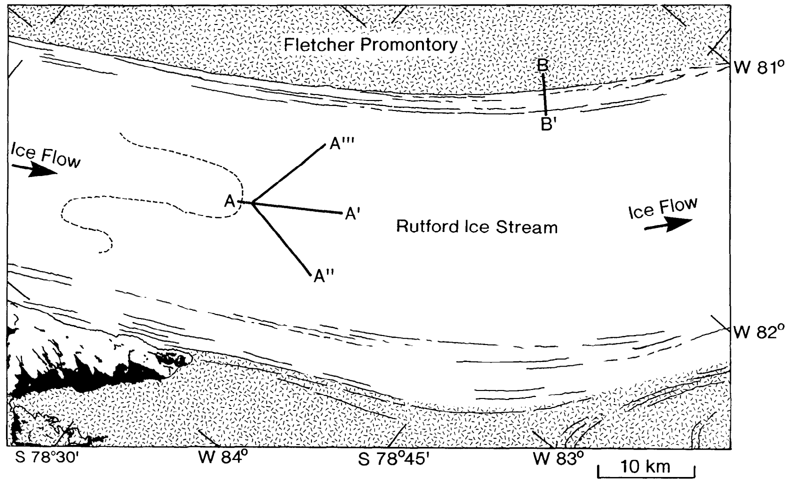

Figure 3. Locations of kinematic GPS profiles on Rutford Ice Stream and Ronne Ice Shelf. Dotted line marks the limit of flexure determined by *Smith* [1991] and hatching marks the approximate extent of the grounded marginal ice.

tainty of ±5 cm. These sources of error are independent and so in total give an uncertainty of ±6 cm.

Tidal Correction

Each profile collected cannot be considered to represent a "snap shot" of the ice sheet since each took around 30 min to collect and some tidal change would have occurred during that period. To correct for this effect I have used a tidal prediction based on the analysis of a long-term tiltmeter record by *Stephenson* [1984] which was scaled using gravimeter measurements [*Doake*, 1992]. The analysis includes the four main tidal constituents (O_1, K_1, M_2, S_2) which accounted for around 84% of the amplitude of the measured signal (total amplitude of 3.64 m). The tidal prediction of amplitude should thus be no more than 17% in error. Using a reconstitution of these species I calculated a tidally corrected displacement, d, between profiles, at each point along the track, where d is defined as

$$d = \frac{e - e'}{p - p'} \tag{5}$$

where e and e' are the observed elevations at a particular point along the profile on the first and second visits. The predicted tidal heights at the time that each measurement was made are p and p'. Thus d represents the amplitude of the tidal displacement between profiles normalized to the maximum tidal displacement predicted by the model. Hereinafter, for the sake of brevity I refer to profiles of d as tidal profiles.

In this analysis there is a tacit assumption that the tidal correction applies uniformly to the whole profile. Any failure of this assumption would be manifested by a disagreement between independent tidal profiles. There are two simple scenarios under which this might occur: there is a significant change in the tidal phase over the area covered by the profiles; the response of the ice shelf to the tidal forcing is not instantaneous but is delayed.

Interpretation of Corrected Tidal Displacement Profiles

Figure 5 shows tidal profiles for lines A-A', A-A'', and A-A'''. Four separate profiles were collected along lines A-A' and A-A'' allowing the two independent tidal profiles to be calculated. Unfortunately, only three successful profiles were obtained over A-A''', so that the two tidal profiles presented for A-A''' are not entirely independent.

The tidal profiles along lines A-A' and A-A'' show the behavior expected by the model, with the flexing of the hinge zone extending 10 km onto the floating ice shelf. The flexing would be monotonic if the observation noise of ±6 cm were removed. The tidal profile for line A-A''', however, is different from the others since it has a maximum between 8 and 8.5 km. If we extrapolate the line A-A''' toward Fletcher Promontory it intersects the margin of Fletcher Promontory at around 17.5 km (Figure 3). The displacement maximum is thus roughly halfway between the two points of grounding. I conclude that flexing along the line beyond the displacement maximum is dominated by the Fletcher Promontory grounding zone and not the Rutford Ice Stream grounding zone. This interpretation is confirmed by the amplitude of the tidal profile which has a maximum that is less (a factor 0.57 and 0.63) than for those along lines A-A' and A-A'', so even at the point of maximum displacement the ice shelf is not freely floating but is significantly damped by the combined restraint from both grounding lines. The measured amplitude of damping (0.57 and 0.63) is roughly consistent with the superposition of two flexing profiles given in Figure 5a, each damping the movement at the midpoint by a factor of 0.83 (0.83^2=0.69). The first 4 km of these profiles will not be significantly affected by the Fletcher Promontory grounding line (being at least 13.5 km away from it) and so only these 4 km will be used in the elastic beam analysis that follows.

Along the lines A-A' and A-A'' the agreement between the two independent tidal profiles is good (Figures 5a and 5b), and neither effect mentioned in the previous section is likely to be important. Along the line A-A''', however, there is a slightly altered shape between the independent tidal profiles (Figure 5c). The maximum itself alters position

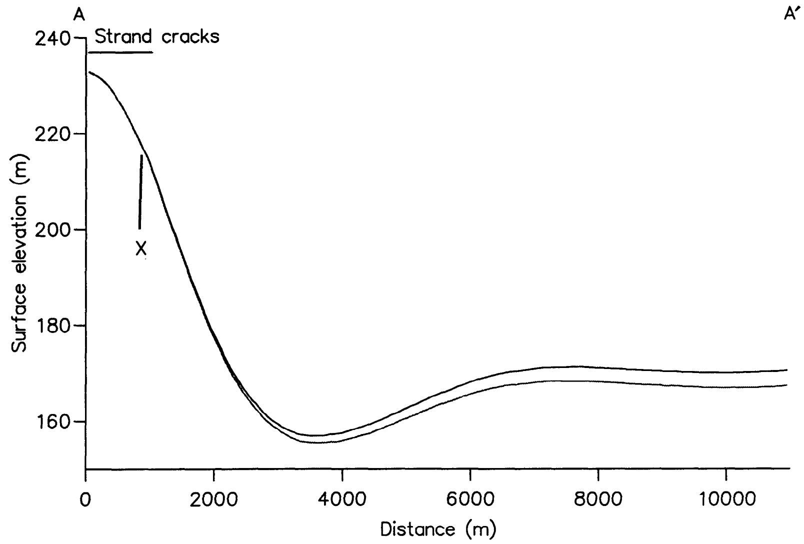

Figure 4. Surface elevation profiles along A-A'. Two profiles are plotted showing the tidal displacement over floating ice shelf. X marks the point at which the three lines diverge.

from x = 8 km to x = 8.5 km and its amplitude falls by 0.2 m. Smith and *Doake* [1995] show that the bedrock topography is very complex, and it is certainly possible that a change in tidal phase along the profile is responsible for this small change in shape of the tidal profile.

Parameter Fitting

The fitting of observations using a theoretical model tuned by key variables is best done by a technique that is repeatable and yields an estimate of the constraint on the tuned variables [*MacAyeal*, 1993]. For the simple problem present here, I adopt a parameter space method [*Anderson and Burt*, 1985, p. 322], in which the root mean square (rms) difference between the tidal profile and the predicted deflection is calculated for a range of values of A_0 and β. The optimal values for the tuned parameters are given by the position in parameter space of the minimum rms mismatch and the uncertainty in the tuned parameters is given by the half width of the "well." If the model is a good description of the physical processes at work, then the smallest rms mismatch should be similar to the observational error.

Figure 6 shows the A_0-β space variation of the rms difference between the displacement profile A-A' and (3). This figure shows that there is only one minimum in A_0-β space, thus indicating only one possible solution. Figure 5a shows a comparison of the observations and the model calculated using the best values of A_0 and β. A similar analysis has been done for each of the corrected tidal profiles and the derived parameters are shown in Table 2.

Smith and Doake [1995] give the ice shelf thickness in this area to be around 1550 m and not varying by more than 100 m (6%). It is thus reasonable to assume that the derived β should be constant within 5% for the profiles (4). Table

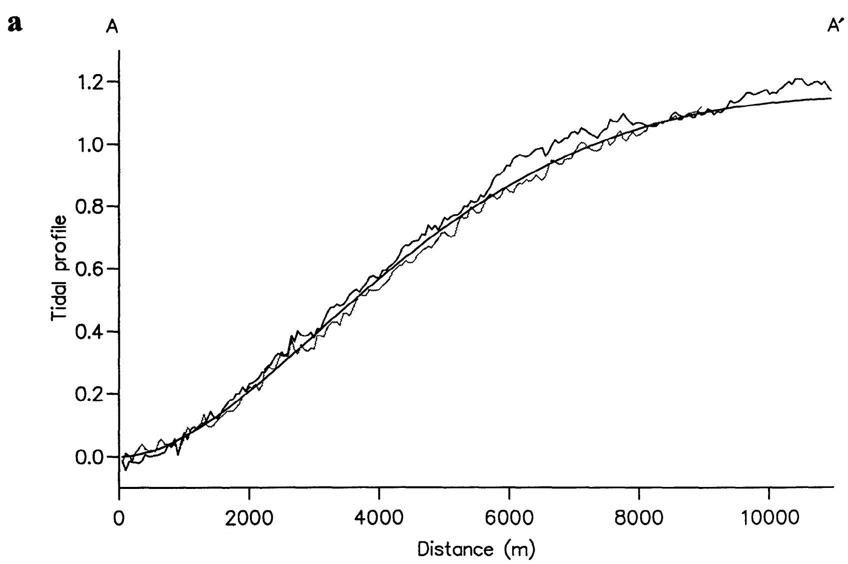

Figure 5. Tidal profiles for (a) A-A', (b) A-A'', and (c) A-A'''. Pecked lines are observed data and solid lines the best fit model equation.

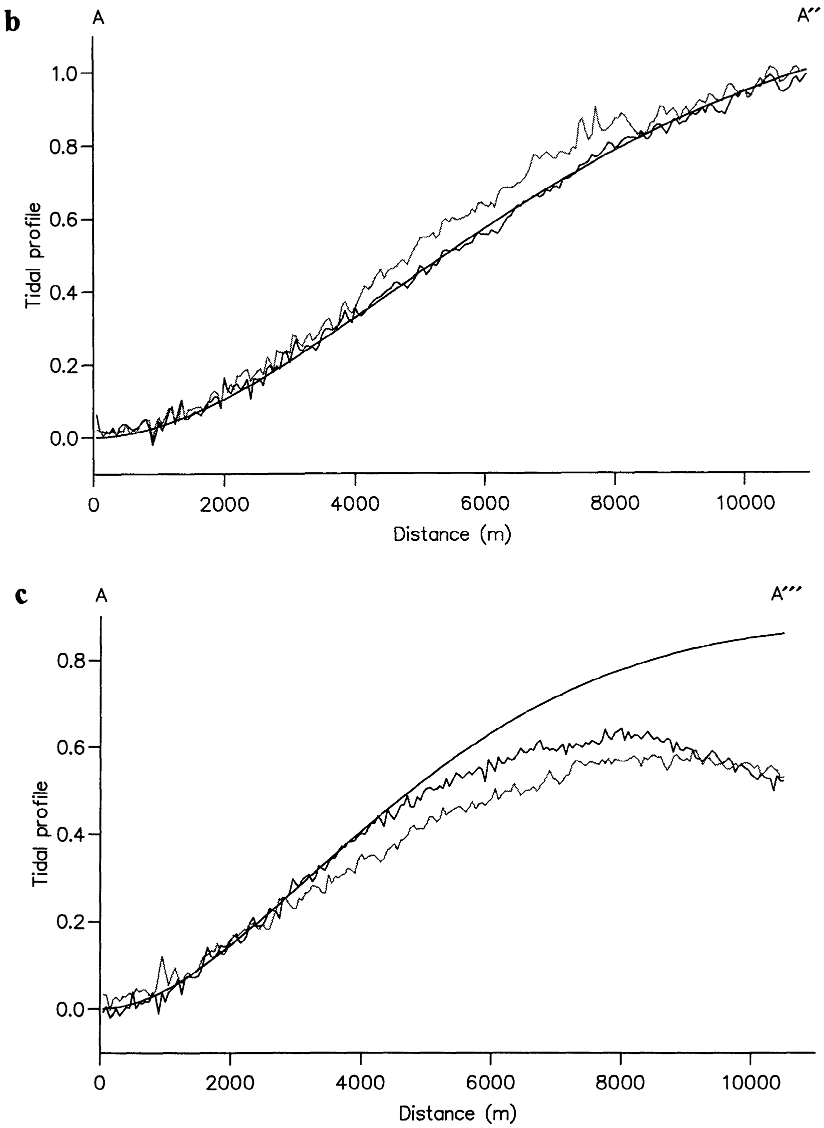

Figure 5. (continued)

2 shows that the derived values of β are not well enough constrained to test this hypothesis. A representative value of β from the grounding line sites is taken to be the mean of the first four measurements listed in the table. The last two were discarded since the data do not constrain the fitting parameters well, a result of being too short to cover enough of the curve to constrain the model. The mean values are $\beta = (2.43 \pm 0.43) \times 10^{-4}\ \mathrm{m}^{-1}$ and $A_0 = (3.9 \pm 0.2)$ m, where the quoted uncertainties are the standard errors around the mean of the derived values which agree well with the uncertainties determined by the parameter fitting technique. The value of A_0 agrees with the tidal amplitude of 3.62 m derived by *Doake* [1992] from gravity measurements, although the likely errors that could be attached to his figure are unclear.

Using the derived value of β and (4) I find E to be in the range 0.57 GPa to 2.4 GPa (1.1 GPa using the center value of β). These values are completely consistent with those presented by *Smith* [1991] who reanalyzed *Stephenson's* [1984] tilt measurements. The correspondence between Smith's value and that derived here lends weight to Smith's reinterpretation of Stephenson's observations.

Ronne Ice Shelf Shear Margin

A similar experiment to that at the Rutford Ice Stream grounding zone was performed in the shear margin between Ronne Ice Shelf and Fletcher Promontory (profile B-B' in Figure 3). At this location there were many open crevasses, and for reasons of safety the "rover" antenna was mounted on a skier rather than snowmobile, causing a small increase in the noise on the profiles. The tidal profiles (Figure 7 and Figure 8) show that the flexing is smooth and similar in style to that from Rutford Ice Stream grounding zone. *Vaughan* [1995] discussed the overall shape noting that the profile does not have the stepped appearance that might be expected to result from full thickness faulting of the type suggested by *MacAyeal et al.* [1986]. He concluded that no such faults were present in the ice shelf at this location. The same analysis and parameter fitting has been performed on these data, and the results are shown in Table 2.

Unfortunately, no coincident measurements of ice thickness were made for profile B-B'. Two airborne radar sounding flights, however, crossed the shear margin around

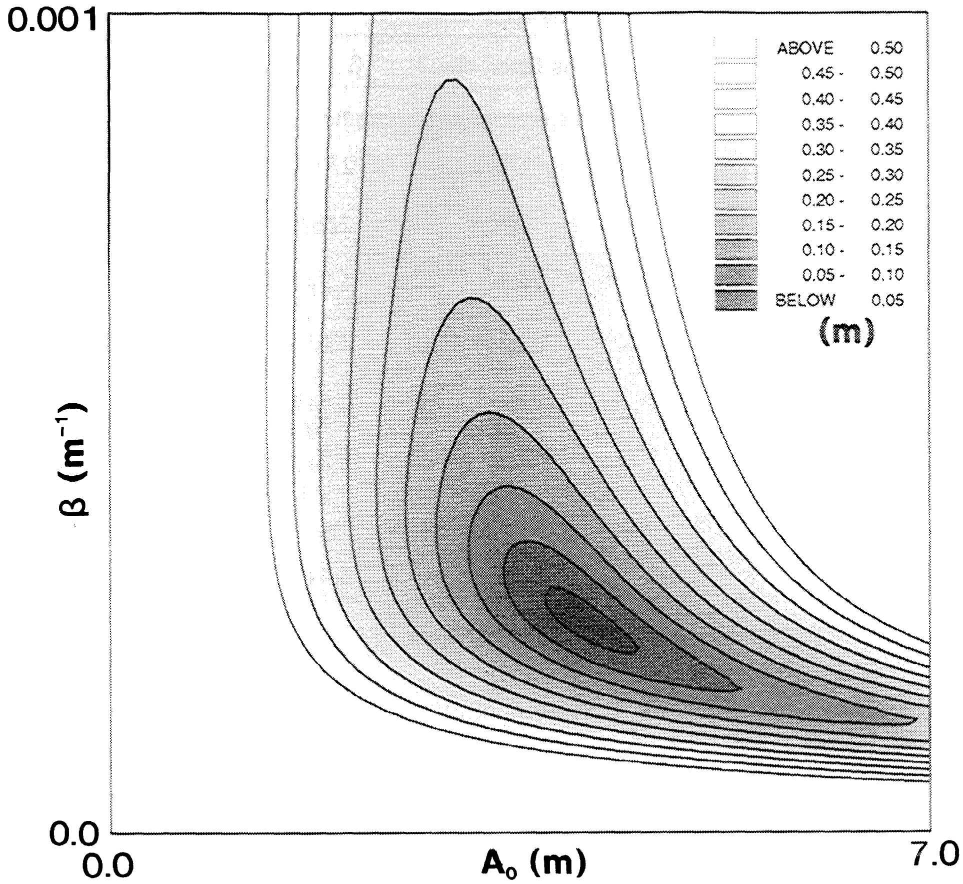

Figure 6. The rms mismatch in meters between model and tidal profile for profile A-A' in the grounding zone of Rutford Ice Stream as a function of amplitude (A_0) and β.

5 km and 13 km downstream of the present line and showed that across the 1.5 km shear margin the ice thins from 1450 m on the ice shelf to 700 m on the promontory (C. S. M. Doake, unpublished data, 1993). Within the shear margin itself the basal radar echo was obscured by surface clutter from crevassing, and so the ice thickness is not available. At present the data are insufficient to warrant a more complex model including a variable thickness beam, and so I suggest it is reasonable to take the thinnest point as representative. With ice 700 m thick (4) gives a value for $E = (0.5 \pm 0.4)$ GPa. This is consistent with the values derived for the Rutford Ice Stream grounding zone. If this is an appropriate value for the ice thickness then there is no significant strain softening of the shear margin for tidal flexing. If, however, the representative ice thickness were taken to be closer to 1450 m then E would be 0.05 GPa, which might indeed indicate some strain softening.

The derived tidal amplitude (A_0) in this area is smaller than at the grounding line 30 km upstream. This is not surprising as the tidal amplitude is amplified close to the grounding zone compared to values further out on the ice shelf [*Doake*, 1992].

Application of Elastic Beam Model to Other Data sets

As already noted, the literature contains the results of several investigations of tidal flexure of ice shelves, some of which have already been successfully modeled using the elastic beam model. Here I shall reinterpret these observations using the parameter space fitting technique presented above. The difference in approach from the original studies is that the elastic modulus is not assumed to be known. For each site I give only a brief summary of the local conditions, and since to determine the elastic modulus we require the ice thickness I discuss ice thickness measurements that will be used later when a comparison is made between the data sets.

Doake Ice Rumples, Antarctica

Ice rumples are areas where a floating ice shelf overrides a bedrock shoal that is at such a depth that the ice shelf can maintain forward flow. Doake Ice Rumples (Figure 1) are within Ronne Ice Shelf and have an area of 1700 km^2. *Smith* [1991] presented data from tiltmeters from five sites along a profile perpendicular to the upstream grounding zone of Doake Ice Rumples. He analyzed his tiltmeter records to obtain the amplitude of the semidiurnal (primarily M_2) component as a function of distance from the crest of the ice rumples and used the elastic model to fit a flexing profile to the data. In his analysis, Smith adopted a value of elastic modulus derived by extrapolating to tidal frequencies the variation of E with loading frequency given by *Sinha* [1978]. The model fits the data well, but the method of analysis does not provide the best value of E or give an indication of the likely uncertainty. Smith noted that the greatest problem in

Table 2. Results From Parameter Fitting

	rms Error, cm	β, 10^{-4}/m	A_0, m
	Rutford Ice Stream grounding line		
A-A'	2.2	2.7±0.4	4.0+0.5 -0.3
A-A'	1.7	2.5±0.4	4.1+0.8 -0.4
A-A''	1.8	1.7+0.4 -0.3	4.0+1.4 -0.6
A-A''	2.2	2.1±0.4	3.7+1.4 -0.6
A-A'''	1.4	2.5+2.4 -0.6	3.1+2.1 -1.0
A-A'''	1.8	4.4+2.8 -1.7	1.3+2.9 -0.4
	Ronne Ice Shelf Shear Margin		
B-B'	2.6	5.4+2.7 -1.5	2.2+1.6 -0.4
	Published Data		
Doake Ice Rumples	2.3×10^{-5} (tangent of tilt)	3.4±0.7	2.8±0.7*
Bach Ice Shelf	3.1	11.0+2.5 -1.7	1.18+0.15 -0.10
Ekström Ice Shelf	3.75×10^{-5} (tangent of tilt)	11.2±0.7+	1.9+1.9 -0.4
Jakobshavns Glacier	1.0	17.0+4.0 -2.0	0.34 ±0.03†

*M_2 tidal range.
†Since this is not the maximum tidal deflection, this value is not the tidal amplitude.

analyzing the tidal flexure of ice shelves arises from not knowing the correct rheology of ice at tidal frequencies.

The tidally induced tilt of the elastic beam, $T(x, t)$ is derived by differentiating (3) with respect to x.

$$T(x,\ t) = \frac{\partial w}{\partial x} = 2A(t)\beta e^{-\beta x}\sin\beta x. \qquad (6)$$

For this study I have reanalyzed Smith's M_2 amplitude data using the parameter space method described above; the resulting profile is shown in Figure 9. The data constrain the model and yield a value of β=3.4 x 10^{-4} m^{-1} close to that used by Smith but giving a marginally better fit to the data (compare Smith's Figure 8). The value of A_0 (2.8 ± 0.7) also agrees well with the value obtained by *Doake* [1992] from Smith's data (2.74 m). Smith estimates his M_2 amplitudes to have an uncertainty of around 20 µrad which agrees well with the best rms mismatch, calculated in terms of the tangent of the tilt angle, between data and model which is 22 µrad. *Smith* [1986] also reports radar sounding measurements along the profile which indicate the ice thickness to be 1000 m.

Bach Ice Shelf, Antarctica

Bach Ice Shelf (Figure 1) is on the west coast of the Antarctic Peninsula close to the climatic limit for ice shelves [*Doake and Vaughan*, 1991] in an area of high snow fall. It

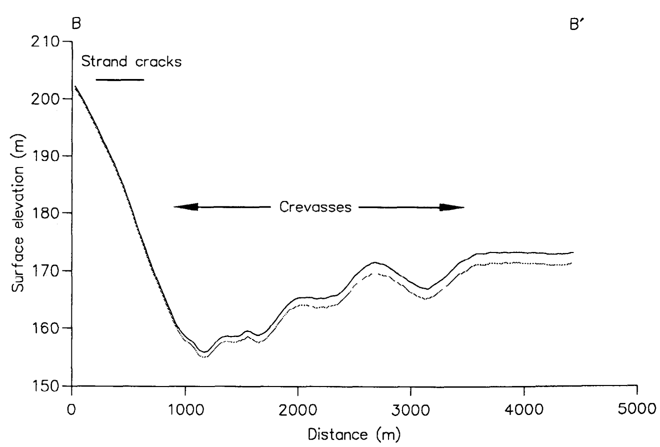

Figure 7. Surface elevation profiles along B-B'. Two profiles are plotted showing the tidal displacement over floating ice shelf.

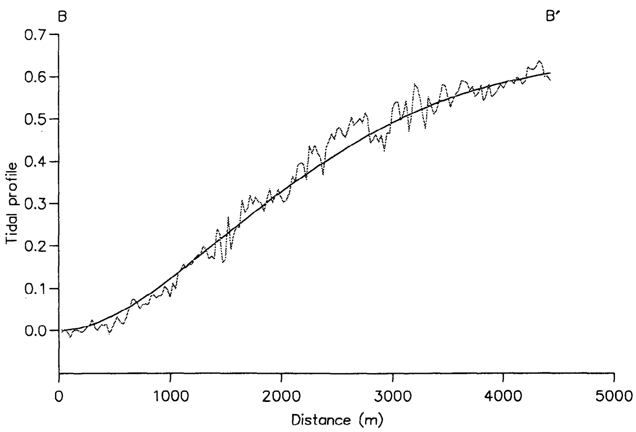

Figure 8. Tidal profiles for Ronne Ice Shelf shear margin (B-B'). Pecked line is the observed data and solid line the best fit model equation.

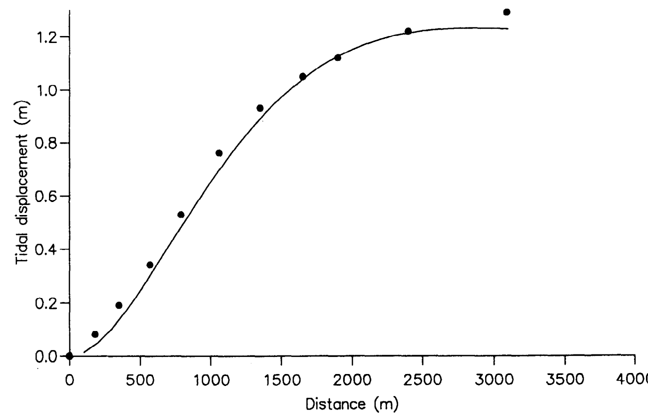

Figure 10. Tidal displacement profiles from Bach Ice Shelf. The points mark observations and line the best fit model equation.

may well have the same unusual regime as its neighbor Wilkins Ice Shelf, which is largely sustained by in situ accumulation and is for the most part infiltrated by seawater [*Vaughan et al.*, 1993].

Optical measurements of tidal flexure on a 4-km line across the shear margin have been made on Bach Ice Shelf, Antarctica, at approximately S72°13' W 071°51' (A. Woodruffe, unpublished data, 1976). The elevations of 11 stakes were made at 12 intervals during the tidal cycle. The maximum displacement of around 130 cm has been calculated from observations at high and low tide (Figure 10). The displacement data have been modeled using the displacement (3) and the parameter space fitting technique, with results shown in Table 2, both A_0 and β being well constrained by the data. Woodruffe estimated the observational uncertainty to range from 1 to 6 cm. This compares well with the minimum rms error of 3.5 cm given by the parameter fitting technique. Unfortunately, there are no coincident ice thickness measurements available across this line, but nearby airborne radio echo sounder data indicate a likely thickness of 250 m [*Crabtree*, 1983].

Ekström Ice Shelf, Antarctica

Kobarg [1988] collected tiltmeter records over the unnamed ice rumples at S 70°32' W 008° 31' on Ekström Ice Shelf, Antarctica (Figure 1). He analyzed these records for the amplitude and phase of the main tidal constituents, O_1, K_1, M_2 and S_2. I have assumed that the flexing limit over the ice rise coincides with the summit of the ice rise [*Kobarg*, 1988, Figure 126]. The parameter space fitting technique has been used to model the four tidal constituents given by Kobarg separately using (6). Only the stations on the upstream side of the crest of the ice rumple have been used. The analyses from Georg von Neumayer station were also included, although this site is not exactly collinear with the rest of the sites giving a total of six points for each constituent. The rms error is determined in terms of the tangent of the tilt angle.

The derived values of β show good agreement between constituents. However, Kobarg's estimates of the uncertainties in the amplitudes are considerably lower (at approximately 5 x 10^{-6}) than the model/data mismatch (4 x 10^{-5}). This may be due to underestimated error limits or an inapplicable model.

Using Kobarg's Figure 9.4 [*Kobarg*, 1988, p. 126], I estimate the ice thickness to be 150-200 m, although, as indicated, the thickness of uncrevassed ice might be considerably less. This thickness is supported by the radar sounding of *Thyssen and Grosfeld* [1988].

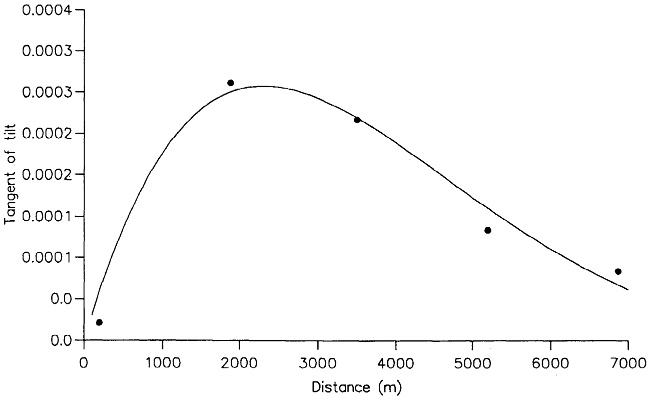

Figure 9. Tidal tilting profiles for Doake Ice Rumples. Points are M_2 tilt amplitudes determined by *Smith* [1991] and the line is the best fit model equation.

Jakobshavns Glacier, Greenland

Jakobshavns Glacier is the largest outlet glacier on the West Greenland coast. Near the calving front ice velocities of up to 7 km per year are reached, the surface is very heavily crevassed, and considerable surface melting occurs. The glacier extends between 10 and 15 km beyond the grounding zone [*Echelmeyer et al.*, 1991] and may be considered as an embayed ice shelf.

Lingle et al. [1981] surveyed the vertical displacements of targets along two profiles perpendicular to the lateral margin of the floating part of the Jakobshavns Glacier. The measured flexure was interpreted in terms of the elastic beam model. Having assumed an elastic modulus of 8.8 GPa, Lingle et al. found that the agreement was not good, and so they postulated an effective elastic thickness of between 21% and 40% of the actual ice thickness. As the model/data agreement was still poor, he also included a viscoplastic term in his constitutive relation. This improved the fit but he still had to use a reduced ice shelf thickness.

I have used the data given by Lingle et al. in their Table 2 for the profile A-E and the data from the three observation times averaged before fitting them to the displacement equation (Figure 11). The results of the parameter space fitting technique are given in Table 2. Lingle et al. estimate the uncertainty on their observations of displacement to be between 4 and 20 cm, and this should be reduced to between 2 and 10 cm by averaging over the observation epochs. The parameter fitting achieves 1.5 cm of rms mismatch. This is perhaps not surprising as there are only five stations across the profile, and the model has enough degrees of freedom to fit the data closely.

It is unclear where Lingle's figure of 750-800 m for the full ice thickness was derived, but the elevation measurements of *Echelmeyer et al.* [1991] suggest that this may have been too large and that an estimate of around 450 ± 50 m would be more reasonable. Although intense crevassing in the surface of the glacier penetrates to a depth of between 40 and 50 m, it is unclear how much this layer can contribute to the elastic thickness. It is unknown whether there are basal crevasses that similarly reduce the elastic thickness. In the absence of any clear value for this reduction in competent thickness I assume it to be 450 m.

Maudheim Ice Shelf, Antarctica

Robin's [1958] optical observations on Maudheim Ice Shelf (Figure 1) were the first to indicate that an ice shelf hinge zone extended into the ice shelf and are included here for completeness. Displacement data have been extracted directly from Robin's Figure 49. Unfortunately, these data do not extend far enough onto the ice shelf to completely cross the hinge zone, and the displacement profile is not complete. Consequently, the parameter space fitting procedure shows that A_0 and β are not at all well constrained. For this reason these data are not included in the comparison of data from different ice shelves.

Harmonization of Site Data

In each of the cases given above the observations have been well matched by the model. And in each case (excepting that from the Ekström Ice Shelf) the rms error derived from the parameter space fitting procedure has been similar to the quoted observational error. In satisfying this requirement the model appears to be a good description of the physical behavior of the flexing.

Equation (4) shows that β is expected to be dependent on both the elastic modulus (E) and the ice thickness (h). If E is constant then plotting derived values of β against $h^{-3/4}$ for each of the sites should give a linear relation. As the ice shelf thickness tends to infinity, the stiffness of the ice shelf becomes infinite and so the spatial wavenumber tends to zero. This condition corresponds to forcing the straight line to pass through the origin. Figure 12 shows that such a single straight line does indeed fit most of the data (Rutford Ice Stream grounding zone, Ronne Ice Shelf shear margin, Doake Ice Rumples, Bach Ice Shelf and Ekström Ice Shelf). Only Jakobshavns Glacier does not appear to fit the pattern. Likely error bounds for β, derived from the parameter fitting technique, are shown. I conclude that the effective elastic modulus is constant for these sites. Its value determined from the gradient of the line is E=(0.88 ± 0.35) GPa. This figure is close to that derived from the values given by Budd and Jacka (0.83 GPa).

The elastic modulus appears constant between sites that have a wide range of surface temperature and composition as suggested by *Budd and Jacka* [1989] who noted that the magnitude of the elastic response is almost independent of temperature and fabric.

For the sake of the intuitive grasp of the result, I offer some comparisons. The elastic modulus derived here suggests that ice deformed at tidal frequencies is an order of magnitude stiffer than many low-density plastics but at least 2 orders of magnitude less stiff than most metals. The elastic modulus derived here (0.88 ± 0.35 GPa) is comparable to that obtained for static loading of polypropylene (1.1-1.6 GPa) [*Kaye and Laby*, 1986].

Although the data discussed by *Sinha* [1978] were obtained in the laboratory and covered a range of loading frequencies that were an order of magnitude higher than the dominant tidal frequency, an extrapolation of the experimental data he presented gives a value that is close to that obtained in this study (1-3 GPa). Closer inspection of his data shows that if it were limited to only granular, as opposed to columnar ice, the agreement would be even closer.

The only data that do not fit the trend line are that from Jakobshavns Glacier. This is despite the model fitting the Jakobshavns Glacier data successfully, and the resultant fit of β being well constrained. The derived value of β, however, suggests a considerably lower ice thickness than has been measured. Lingle et al. had a similar problem with their interpretation of the data. They decided that they should consider an effective ice thickness that took account of weakening due to surface and basal crevassing. If I turn the problem round, assuming that the elastic modulus for Jakobshavns Glacier is the same as the other sites, then the derived value of β will lie on the line in Figure 12, if the effective ice thickness is around 150 m. This is considerably less than the estimate of total ice thickness 450 m on the floating ice by *Echelmeyer et al.* [1991]. This disparity is possibly due to a combination of ice shelf thinning near the margin and surface and basal crevassing that reduces the strength of the ice column.

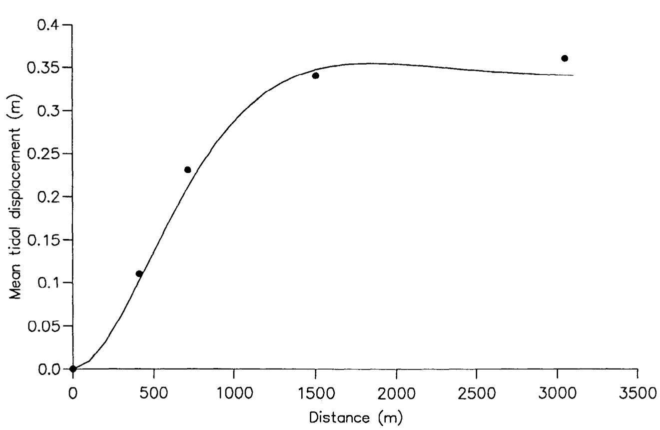

Figure 11. Mean tidal displacement profiles from Jakobshavns Glacier [*Lingle et al.*, 1981, profile A-E]. Points mark the observations and lines the best fit model equation.

Discussion

Grounding Line Migration

All the examples given above are from locations where the bedrock beneath the grounding zone is relatively steep and

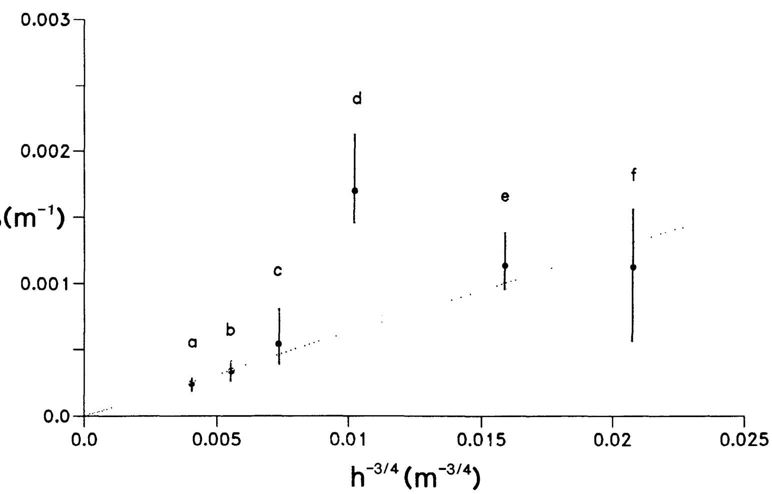

Figure 12. Variation of derived β with measured ice shelf thickness. Letters indicate a, Rutford Ice Stream grounding line; b, Doake Ice Rumples; c, Ronne Ice Shelf shear margin; d, Jakobshavns Glacier; e, Bach Ice Shelf; f, Ekström Ice Shelf.

the grounding line (point of contact with the bed) does not migrate during the tidal cycle. With a shallow bedrock slope the grounding line migrates during each tidal cycle and the bending stresses are reduced. If the migration range exceeds the natural flexing length of the ice sheet then the bed geometry will dominate the form of ice sheet bending. Although the simple elastic beam analysis used above is adequate for the case of a steep bed, it would be have to be modified for the analysis of flexing through a low bed slope grounding line to include a moving point of contact.

Tidal Dissipation at Grounding Lines

Doake [1978] attempted to evaluate the dissipation rate of tidal energy by ice shelves and concluded that they might account for as much as a third of the energy lost by the rotational system of the earth and moon. The major uncertainty in Doake's calculation was, however, the choice of the constitutive equation. He assumed that the response of ice shelves to tidal forcing was by creep deformation, the same type of deformation that accounts for the steady flow of ice from the center to the edge of the ice sheet. It is now clear that the creep deformation considered appropriate by Doake only develops some period after loading. *Hutter* [1983, p. 83] suggests that even for quite large stresses (700 kPa) and warm temperatures (-4.8°C) tertiary creep may not develop until 100 hours after loading. With a loading due to tidal forcing of around 6 hours it is unlikely that tertiary creep could ever develop.

The results presented here confirm that the present observations of the tidal deformation of ice shelves can be explained by conservative elastic deformation. The use of such a less dissipative, or even conservative constitutive relation, would have radically reduced Doake's estimate of the dissipation rate. Indeed, if the rheology is elastic (conservative) then the dissipation of tidal energy in the ice itself will be negligible.

The measurement presented here cannot, however, conclusively point to a conservative rheology. In order to measure directly the energy dissipation, we must make simultaneous measurements of the forcing (the seawater pressure at the ice shelf base) and displacement of the ice shelf during the tidal cycle. A non-conservative ice rheology would lead to a time delay between these two cycles. Other proxies might also be considered for the seawater pressure at the ice shelf base, for example, the level of water in a borehole penetrating the ice sheet, or a combination of seabed pressure and ice surface elevation.

Summary

I have presented a new method of obtaining continuous tidal profiles in ice shelf hinge zones and shown the results collected from two locations. Adopting a model already described, I have shown using a nonsubjective and reproducible parameter fitting technique that a model of ice flexure based on unmodified elastic beam theory can adequately explain these profiles. Using the same model and technique I have shown that almost all of the data from previous studies can be explained by the same model without modification. In all but one case the model fits the data within the quoted observational error and so can justifiably be claimed as a good physical description of the physical process.

I find that a single elastic modulus (E = 0.88 ± 0.35 GPa) adequately fits all the sites with the exception of Jakobshavns Glacier. This value of E, however, represents an average value for the whole ice column and even though there is no evidence for variation of elastic modulus with temperature, there may be a variation due to ice density or overburden pressure through the ice column. Furthermore, the model has assumed that the neutral surface, along which the tidal flexing causes no extension or compression, lies halfway through the ice shelf. A variation in elastic modulus could displace the neutral surface according to the lowest energy state and so would also alter my estimate of the average elastic modulus. At present I cannot model this effect since there is no indication of the likely variation in the elastic modulus with these parameters. For the present study I have been content to derive the average elastic modulus.

The single elastic modulus also appears independent of structural style, since it has been shown to apply to ice flowing seaward across a grounding line (Rutford Ice

Stream, grounding line), ice flowing parallel to a grounding line (Rutford Ice Stream, shear margin and Bach Ice Shelf) and ice flowing landward across a grounding line (Doake Ice Rumples and Ekström Ice Shelf). In each case the tidal flexure was modeled without consideration of the steady state dynamics, or state of the longitudinal stresses in the ice. It thus seems reasonable to conclude that tidal flexing can be considered in isolation from the ice flow, and as a perturbation on the steady state regime.

Doake [1978] estimated that the dissipation of tidal energy by ice shelf margins might be up to a third of the energy lost from the Earth-Moon rotational system. He assumed that the deformation in response to the tidal forcing was by creep, a non-conservative mode of deformation. Here I have shown that there is no strong evidence to suggest that this deformation occurs by creep and that a simpler description using an elastic rheology can adequately describe the observational data. I suggest that Doake's figure is suspect but can only be confirmed or denied conclusively by direct measurement of phase lag between forcing and response.

Acknowledgments. My thanks to the NERC Geophysical Equipment Pool who loaned the GPS receivers, Crispin Day for his tireless assistance in the field, and Chris Doake and Andy Smith, who gave much invaluable advice during the research and considerable improvements to the text. Reviewers, R. Bindschadler, B. Hanson, and C. Raymond have suggested considerable improvements.

References

Anderson, M. G., and T. P. Burt, *Hydrological Forecasting*, 604 pp., John Wiley, New York, 1985.

Budd, W. F., and T. H. Jacka, A review of ice rheology for ice sheet modelling, *Cold Reg. Sci. Technol.*, *16*, 107-144, 1989.

Crabtree, R. D., Alexander Island, Ice Thickness Map, scale 1:500,000, Br. Antarct. Surv., Cambridge, 1983.

Doake, C. S. M., Dissipation of tidal energy by Antarctic ice shelves, *Nature*, *275*, 304-305, 1978.

Doake, C. S. M., Gravimetric tidal measurements in Filchner-Ronne Ice Shelf, *Filchner-Ronne Ice Shelf Programme Report No. 6*, pp. 34-39, Alfred Wegener Institut, Bremerhaven, Germany, 1992.

Doake, C. S. M., and D. G. Vaughan, Rapid disintegration of Wordie Ice Shelf in response to atmospheric warming, *Nature*, *350*, 328-330, 1991.

Echelmeyer, K., T. S. Clarke, and W. D. Harrison, Surficial glaciology of Jakobshavns Isbrae, West Greenland, Part 1, Surface morphology, *J. Glaciol.*, *37*, 368-382, 1991.

Goldstein, R. M., H. Engelhardt, B. Kamb, and R. M. Frolich, Satellite radar interferometry for monitoring ice sheet motion: Application to an Antarctic ice stream, *Science*, *262*, 1525-1530, 1993.

Hetényi, M., *Beams on Elastic Foundations*, University of Michigan Press, Ann Arbor, 1946.

Hofmann-Wellenhof, B., H. Lichtenegger, and J. Collins, *GPS Theory and Practice*, 323 pp., Springer-Verlag, New York, 1992.

Holdsworth, G., Flexure of a floating ice tongue, *J. Glaciol.*, *8*, 385-397, 1969.

Holdsworth, G., Tidal interaction with ice shelves, *Ann. Geophys.*,*33*, 133-146, 1977.

Hutter, K., *Theoretical Glaciology*, 510 pp., D. Reidel, Norwell, Mass., 1983.

Kaye, G. W. C., and T. H. Laby, *Tables of Physical and Chemical Constants*, 477 pp., Longman, New York, 1986.

Kobarg, W., The tide-dependent dynamics of the Ekström Ice Shelf, Antarctica, *Ber. Polarforschung 50*, 1-164, 1988.

Lingle, C. S., T. J. Hughes, and R. C. Kollmeyer, Tidal flexure of Jakobshavns Glacier, West Greenland, *J. Geophys. Res.*, *86*, 3960-3968, 1981.

MacAyeal, D. R., A tutorial on the use of control methods in icesheet modelling, *J. Glaciol.*, *39*, 91-98, 1993.

MacAyeal, D. R., S. Shabtaie, C. R. Bentley, and S. D. King, Formulation of ice shelf dynamic boundary in terms of a coulomb rheology, *J. Geophys. Res.*, *91*, 8177-8191, 1986.

McAdoo, D. C., J. G. Caldwell and D. L. Turcotte, On the elastic-perfectly plastic bending of the lithosphere under a generalised loading with application to the Kuril Trench, *Geophys. J. R. Astron. Soc.*, 11-26, 1978.

Minkle, D. H., Kinematic GPS land survey - Description of operational test and results, *J. Surv. Eng.*, *115*, 121-137, 1989.

Remondi, B. W., Global positioning system carrier phase: Description and use, *Bull. Geod.*, *59*, 361-377, 1985.

Robin, G. de Q., Glaciology III, seismic shooting and related investigations, in *Norwegian-British-Swedish Antarctic Expedition, 1949-52, Scientific Results, Vol. V,* Norsk Polarinstitut, Oslo, 1958.

Sinha, N. K., Short-term rheology of polycrystalline ice, *J. Glaciol.*, *21*, 457-473, 1978.

Smith, A. M., Ice rumples on Ronne Ice Shelf, Antarctica, *Br. Antarct. Surv. Bull.*, *72*, 47-52, 1986.

Smith, A. M., The use of tiltmeters to study the dynamics of Antarctic ice-shelf grounding lines, *J. Glaciol.*, *37*, 51-58, 1991.

Smith, A. M. and C. S. M. Doake, Seabed depths at the mouth of Rutford Ice Stream, Antarctica, *Ann. Glaciol.*, in press, 1995.

Stephenson, S. N., Glacier flexure and the position of grounding lines: Measurements by tiltmeter on Rutford Ice Stream, Antarctica, *Ann. Glaciol.*, *5*, 165-169, 1984.

Thyssen, F., and K. Grosfeld, Ekström Ice Shelf, Antarctica, *Ann. Glaciol.*, *11*, 180-183, 1988.

Turcotte, D. L., and G. Schubert, *Geodynamics Applications of Continuum Physics to Geological Problems*, 450 pp., John Wiley. New York, 1982.

Vaughan, D. G., Investigation tidal flexure on an ice shelf using kinematic GPS, *Ann. Glaciol.*, in press, 1995.

Vaughan, D. G., D. R. Mantripp, J. Sievers and C. S. M. Doake, A synthesis of remote sensing data on Wilkins Ice Shelf, Antarctica, *Ann. Glaciol.*, *17*, 211-218, 1993.

Watts, C. B., J. R. Cochran, and G. Selzer, Gravity anomalies and flexure of the lithosphere, 3-dimensional study of the Great Meteor Seamount, *J. Geophys. Res.*, *80*, 1391-1398, 1975.

Whillans, I. M., C. van der Veen, and Y.-H. Tseng, Application of the Global Positioning System in Antarctica, *Antarct. J. U. S.*, *25*(2), 6-9, 1990.

D. G. Vaughan, British Antarctic Survey, Natural Environment Research Council, High Cross, Madingley Road, Cambridge, CB3 0ET, England. (e-mail: dgv@pcmail.nbs.ac.uk)

(Received February 23, 1994; revised August 22, 1994; accepted September 14, 1994.)